CODEX Optical Design and Alignment

Qian Gong*[a], Jeffrey S. Newmark[a], Yeon-Han Kim[b], Marta Casti[c], Lucia Abbo[d], Ji-Hye Baek[b], Su-Chan Bong[b], Jason Budinoff[e], Gerardo Capobianco[d], Kyungsuk Cho[b], Seonghwan Choi[b], Silvano Fineschi[d], Hervé Haudemand[d], Jihun Kim[b], Federico Landini[d], Davide Loreggia[d], Sung-Hong Park[b], Jongyeob Park[b], Nelson L. Reginald[c], Donguk Song[b,f], Heesu Yang[b], Luca Zangrilli[d]

[a]NASA Goddard Space Flight Center, 8800 Greenbelt Road, Greenbelt, MD, 20771, USA;
[b]Korea Astronomy and Space Science Institute (KASI), 776 Daedeok-daero, Yuseong-gu, Daejeon 34055, Republic of Korea
[c]The Catholic University of America at NASA Goddard Space Flight Center, 8800 Greenbelt Road, Greenbelt, MD, 20771, USA
[d]INAF-Astrophysical Observatory of Torino, Via Osservatorio 20 - Pino Torinese, 10025 Italy
[e]Visioneering Space Corp 3380 West Americana Terrace Suite 110 Boise, ID 83706, USA
[f]National Astronomical Observatory of Japan, 2-21-1 Osawa, Mitaka, Tokyo 181-8588, Japan

ABSTRACT

The COronal Diagnostic EXperiment (CODEX) is a Heliophysics mission to measure the density, temperature, and velocity of the electrons in the solar corona with the primary goal of improving our understanding of the physical conditions of the solar wind in the acceleration region. The temperature and velocity measurement requires much higher signal-to-noise ratio than the density measurements. In solar coronagraphs, the diffraction of the solar disk light due to the occulting element is the dominant source of noise. Therefore, to further suppress the diffracted sun light with respect to the existing coronagraphs is a critical element of the CODEX design. To minimize the stray light due to diffraction, the selected optical design is a two-stage standard coronagraph with an external occulter, an internal occulter, and a Lyot stop. What is unique for this design is that a focal mask was inserted at the telescope focal plane. It works together with the field lens suppressing the stray light down by ~ another order of magnitude as compared to a traditional three-stage approach. During the optical design, a Fourier Transform based beam propagation software, i.e., GLAD, was used to model the beam path through the full coronagraph, from the external occulter to the detector array. All diffraction sensitive elements: external occulter, internal occulter, focal mask, and Lyot stop were carefully modeled and optimized. As a result, the requirement of achieving a stray light level which is one order of magnitude lower than F-corona was satisfied. On the other hand, to achieve the final suppression, a precision optical alignment is another must. This paper also presents our creative alignment procedure: using the combination of metrology, precision alignment equipment, and real time diffraction ring monitoring to minimize the diffraction. The final test results show that the suppression ratio (B/B_0) reaches 10^{-11} level, which is equivalent to one order of magnitude lower than F-corona.

Keywords: Solar coronagraph, coronal density, temperature, and velocity, CODEX optical design and alignment

1. INTRODUCTION

All existing imaging solar coronagraph to date only measure the coronal electron density, except the Balloon-borne Investigation of Temperature and Speed of Electrons in the corona (BITSE)[1] that was a prove-of-concept experiment in preparation for the CODEX coronagraph. CODEX will be the first coronagraph on-orbit to measure the coronal electron temperature, velocity, and density all simultaneously[2]. These measurements will answer the critical scientific question: Are there signatures of hot plasma released into the solar wind from previously closed fields? The image data collected by CODEX will also provide new information to understanding the physical mechanisms driving the solar wind acceleration, as well as serve to validate and enable improvements of space-weather models. As mentioned in the abstract, to perform temperature and velocity measurements of the electrons in corona requires much higher signal-to-noise ratio, in other words, much lower stray light. It is well known that the main source of stray light in a coronagraph is the

diffraction. In order to meet the challenge of reducing the instrumental stray light level, a two-stage coronagraph was selected providing more critical planes for further suppressing the diffraction, such as the focal plane of the telescope, internal occulter plane, Lyot stop, etc.

The CODEX coronagraph has the following unique features driven by the science objectives:

1. All externally occulted coronagraphs in the past, such as, SOHO/LASCO-C2[3], STEREO/SECCHI-COR2[4] etc. suppress the diffraction using 3 elements: External Occulter (EO), Internal Occulter (IO), and Lyot stop. To reach the signal-to-noise (S/N) ratio required for coronal temperature and velocity measurements, an additional occulter at telescope focus, i.e., the focal mask, is added. The diffraction analysis, detailed in section 2.2, verifies that the added focal mask indeed further suppresses the diffraction efficiently, which decreases the noise without compromising the signal and the field of view (FOV). Additionally, the vignetting is also reduced, which implies the signal increase. Together, the S/N ratio has been significantly increased.
2. The coronal electron temperature and velocity are measured using the filter-ratio technique (FRT)[5]. The technique retrieves the temperature and velocity information from four density maps at four selected wavelength bands, which is different from common single wavelength band coronagraphs.
3. A polarization camera, utilizing a Sony IMX253MZR CMOS detector, is used to replace the polarizer mechanism[6] used in most coronagraphs. Besides simplicity by eliminating a mechanism, the camera provides polarized brightness (pB) maps in each frame, rather than requiring a time sequence that could allow evolution of features.

It is known that the optical alignment is extremely critical for coronagraph instruments. For CODEX optical alignment, both traditional alignment method and unique real time stray light monitoring are used to minimize the stray light from diffraction and scattering. The detailed alignment process is described in Section 3.

2. OPTICAL DESIGN

The optical design includes two parts: traditional geometric optical design (ray trace) and coronagraph specific diffraction light suppression. The design specification is listed on Table 1.

Table 1. CODEX coronagraph design specification

Parameter	Unit	Capability
Entrance pupil aperture (A1)	mm	50
Effective focal length	mm	111.190
Detector	Sony IMX253MZR	4096 x 3000
Chip size	mm	14.13 x 10.35
Pixel size	μm	3.45
Plate scale	Arcsec / super pixel (2x2 pixels)	13.8
FOV	$R_\odot$	13.65 x 10
FOV	º	3.64 x 2.67
Wavelength range	nm	385 - 440
CODEX final inner FOV cutoff	$R_\odot$	2.75
Inner FOV cutoff at EO	$R_\odot$	1.75
Inner FOV cutoff at IO	$R_\odot$	2.0
Distance from A0 to A1	mm	900
Diffraction suppression	Order of magnitude (3 $R_\odot$ – 8 $R_\odot$)	1 order lower than F-corona

The CODEX camera is a polarization camera. The camera's super pixel is defined as 2 x 2 due to 4 polarization direction on 4 neighboring pixels. The $R_\odot$ on the table is the solar radii as seen from Earth (1AU) that is about the same as the orbit of International Space Station (ISS) that will host the CODEX coronagraph. A0 is the most front aperture that is flashed with the front side of external occulter. A1 is the entrance aperture of CODEX optical system. The distance between A0 to A1 is 900 mm, which is longer than most of the externally occulted coronagraph. The purpose is to relax vignetting and to enhance the signal. Final CODEX inner FOV cutoff is 2.75 $R_\odot$ determined by the focal mask at telescope focus.

2.1 GEOMETRIC OPTICAL DESIGN

CODEX optical system has two stages: a telescope and a relay optics group. What's different from other coronagraph designs is the presence of the focal mask on the field lens, at the focal plane of the telescope. The field lens is a plano-convex lens with its flat surface exactly positioned at the focal plane. The function of the field lens is to reduce the size of the optics after it, and it is commonly used in optical designs. A unique function is given to the field lens in this design: gluing a focal mask at the center of the field lens to increase the diffraction suppression efficiency. It works very well and is detailed in section 2.2.

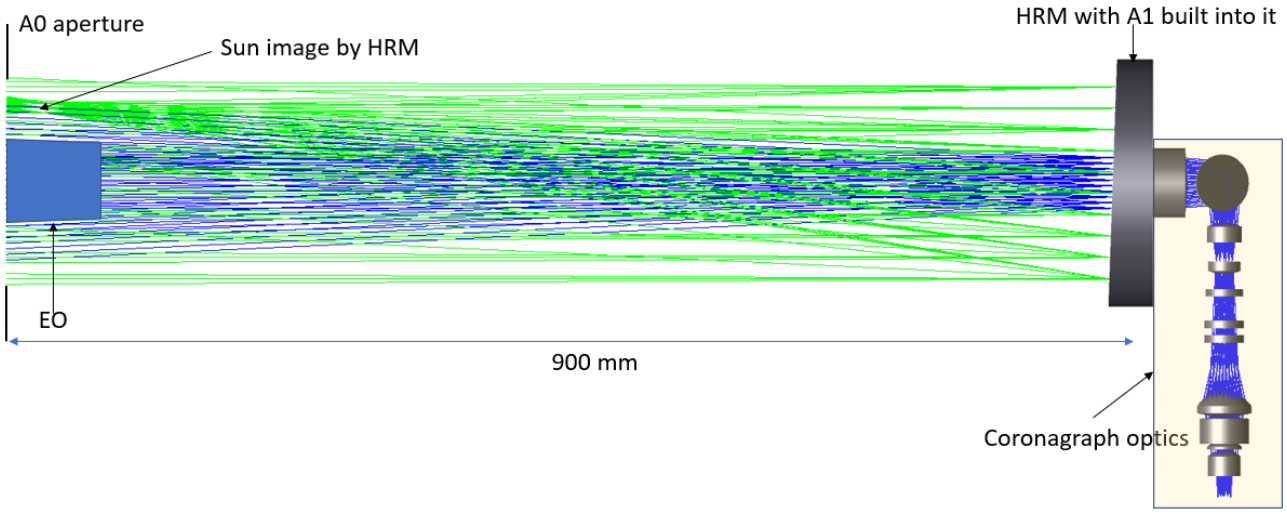

Figure 1. Complete CODEX optical system. Detailed coronagraph system is shown in Figure 4.

The total track of CODEX optical path is longer than most of the coronagraph instruments currently on orbit. It is because the longer separation between A0 and A1 apertures for reducing the vignetting, especially in fields close to inner FOV cutoff. Because of the longer optical track and the limited volume allocated to CODEX on the ISS, the beam path is folded between telescope lens groups. In order to reduce the polarization effect, two-fold mirrors are designed in such a way that their normals are in orthogonal planes. Due to the high S/N ratio requirement the second stage, i.e., the relay lens group, is added to further suppress the residual diffraction. The first element of the relay group is a plano-convex field lens that is located at the telescope focal plane with its flat front surface exactly in telescope focal plane. A circular disk is glued at the center of the field lens to efficiently suppress the diffracted light. To my knowledge, this is the first time an occulter is added at the telescope focal plane. In the diffraction section, we'll explain how this occulter further suppresses the diffraction stray light.

The rest of relay group includes an internal occulter, bandpass filter wheels, Lyot stop, and a 4-element lens group. The camera for CODEX is a polarization camera. Our team member, the Korea Astronomy Space Science Institute (KASI) has developed the CODEX polarization camera using the sensor Sony IMX253MZR as the detector, eliminating the need of a polarizer wheel. However, a filter wheel is needed for the multiple passband requirements. Its elements include 4 narrow bandpass filters and a broad band filter plus several neutral density filters, as well as a few other spectral filters for

additional science[7]. The 4 narrow band filters are used to measure the coronal temperature and velocity, the broad band filter is to measure the density. The central wavelengths and their bandwidths are listed on Table 2.

Table 2. CODEX coronagraph design specification

Filter #	**Central wavelength (nm)**	**Full Width Half Maximum Passband (nm)**	**Purpose**
1	393.5	10	Temperature
2	405.0	10	Temperature
3	398.7	10	Velocity
4	423.3	10	Velocity
5	412.5	50	Rapid Density

The coronal temperature and velocity measurement theory and bandpass filter selection are described by N. Reginald, et al.[5]

The spatial resolution requirement is to meet Nyquist sampling at binned CODEX super pixel shown in figure 2. It is equivalent to 36 cycles/mm. The image quality is evaluated using diffraction-based Modulation Transfer Function (MTF) shown in Figure 3. The MTF in figure 3 indicates the spatial resolution requirement is met, even at inner FOV cutoff at 2.75R (0.73°). This is because CODEX inner FOV cutoff is controlled by the focal mask at the telescope focus. It is well-known that the minimum vignetting is introduced for unocculted fields if the occulter locates at any intermediate focal planes, for example, telescope focus. Even though we still need an IO in place, but the IO does not have to cut as much as field occulter for obtaining optimized diffraction suppression, which means: higher S/N ratio for this application. It will be discussed in detail in next section.

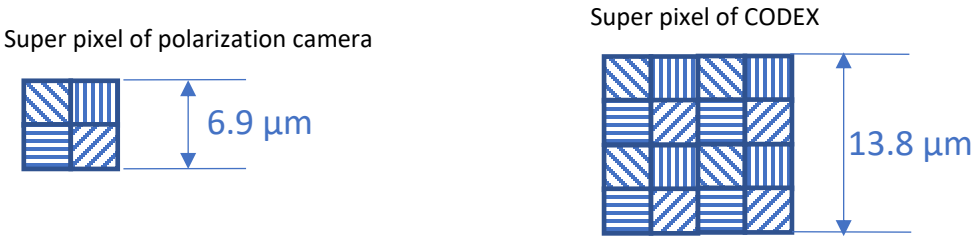

Figure 2. The two super pixel definition are shown above. On the left, the camera vendor has defined camera super pixel (2 x 2) due to polarization masks on pixels, we call it camera super pixel. On the right, we defined CODEX super pixel (4 x 4) that meets S/N demand for the temperature and velocity measurement. To make it clear: 1 CODEX super pixel equals 2 x 2 camera super pixel.

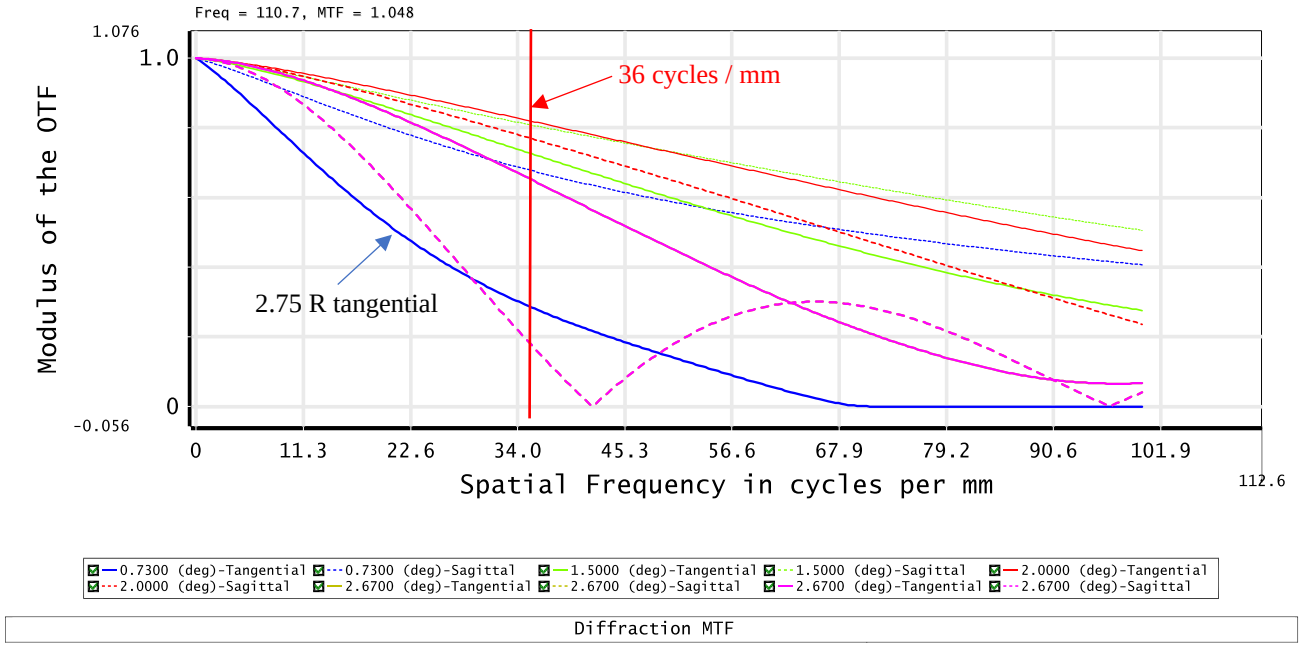

Figure 3. CODEX diffraction based MTF. By definition, if MTF is over 0.1 for any frequency, the object(s) at that frequency is resolved and Nyquist sampled. The vertical red line shows 36 cycles/mm in the plot. All fields meet and beyond the 0.1 MTF required by Rayleigh's criterion[8]. It is even true for tangential 2.75$R_\odot$ that is right at the inner FOV cutoff 2.75$R_\odot$ and suffers most due to vignetting.

2.2 DIFFRACTION SUPPRESSION

A major difference in optical design between coronagraph instruments and other optical instruments is that in coronagraph instruments, diffraction suppression is equally important if not more important than image quality. In this coronagraph, we already trade the spatial resolution (CODEX super pixel) for high S/N ratio. The top-level diffraction suppression requirement is that the final diffraction intensity is an order of magnitude lower than the F-corona brightness within the range that goes from 3$R_\odot$ to 8$R_\odot$.

There are 6 critical elements in this coronagraph that control the diffraction suppression efficiency. These elements are labeled in Figure 4: 1. EO; 2. A1 aperture; 3. A0 stop; 4. Focal mask; 5. IO; and 6. Lyot stop. The A0 stop is used to reduce the scattered light, it is not included in the diffraction section. The initial inner FOV cutoff is controlled by EO and A1. For CODEX it is finally settled at 1.75$R_\odot$. Figure 5 shows the diffraction pattern at the telescope focal plane where the first occulter (focal mask) is placed. In the figure, the inner FOV cutoff determined by EO and A1 is 1.5$R_\odot$. It is realized that the EO cutoff does not impact the side slope of diffraction profile in figure 5. How much diffracted light leaks through depending upon the size of focal mask diameter, assuming the EO length and cone angle keeping the same. For example, if the focal mask's cutoff is 2.75 $R_\odot$, the diffraction intensity in the FOV > 2.75 $R_\odot$ is similar regardless if the EO cutoff is 1.5 $R_\odot$, 1.75 $R_\odot$, or 2.0 $R_\odot$. The trade-off for EO cutoff is the scattered light and vignetting. Smaller EO cutoff may increase the light scattering, but it improves the vignetting near final inner FOV cutoff. For CODEX, the focal mask cutoff is selected at 2.75 $R_\odot$.

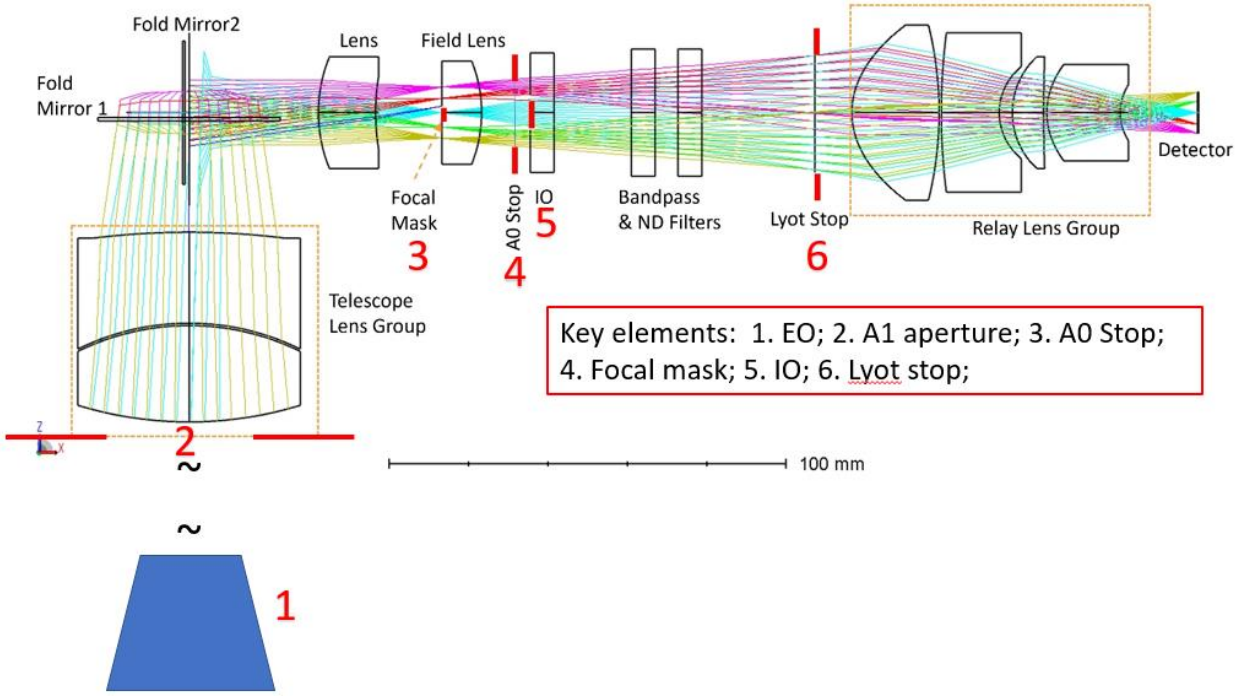

Figure 4. The five elements for minimize solar diffraction are defined and labeled. The element 3, focal mask, is added to efficiently suppress the diffraction further as our novel design.

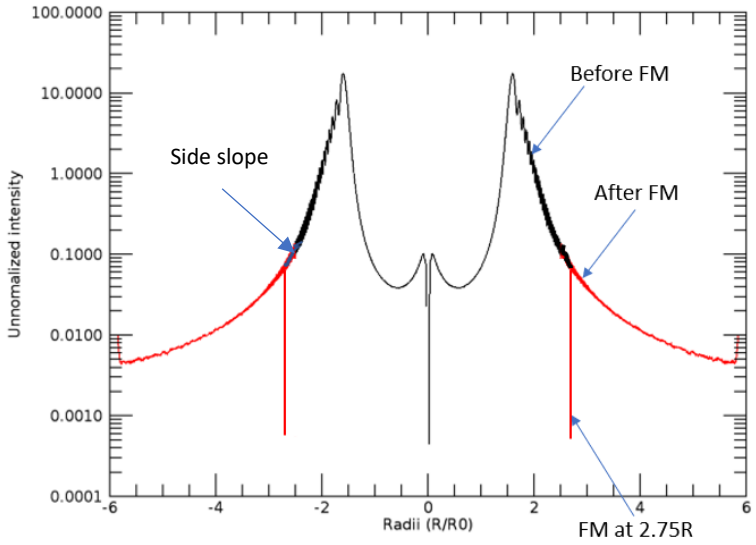

Figure 5. Diffraction intensity profile at telescope focus. The red curve is the diffracted Sun light passing focal mask and leaking into the system.

CODEX field lens not only makes the chief rays from different fields converge to decrease the optical layout size. It also provides a surprise advantage: the field lens with a focal mask concentrates the diffraction light to a sharp ring in the IO plane, which is shown in figure 6. In figure 6 (a), the sharp ring has a peak intensity that is about 3 orders of magnitude higher than the diffracted light anywhere else. (b) is a zoom-in plot near the sharp ring. It is seen that if the IO cutoff at $1.75R_{\odot}$, most of the diffraction is already suppressed. The smaller the IO cutoff is, the less the vignetting nearby final $2.75R_{\odot}$ cutoff at the risk of less efficient diffraction suppression. CODEX IO is finally settled at 2.0 $R_{\odot}$. Note: all

diffraction analysis is performed using a software GLAD, which is a Fast Fourier Transform based physical beam propagation software.

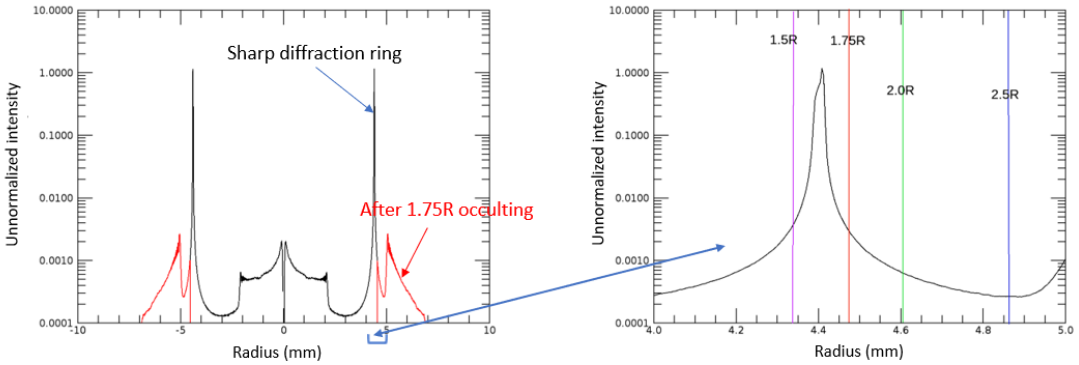

Figure 6. On the left is the diffraction distribution profile at the IO plane. On the right is zoom-in plot in the region that is around the sharp diffraction ring.

The less IO cutoff with respect to final inner FOV cutoff, defined by focal mask, also brings a benefit for spatial resolution near the inner FOV cutoff. Less vignetting means that the crescent aperture near inner FOV cutoff in the middle is wider, which greatly reduces the size of point spread function (PSF) in tangential direction[9]. Compared to other existing coronagraph instruments where the fraction of unvignetted beam is zero at the inner FOV cutoff, for CODEX it already reaches 7%. The improved vignetting also provides benefit to the PSF. It makes the PSF size at $3R_\odot$ within a CODEX super pixel. The $3R_\odot$ is the inner FOV for scientific measurement. In Figure 7, on the left is the fraction of unvignetted beam, which indicating it is 10% at $3R_\odot$. On the right, it shows the PSF size is within a CODEX super pixel.

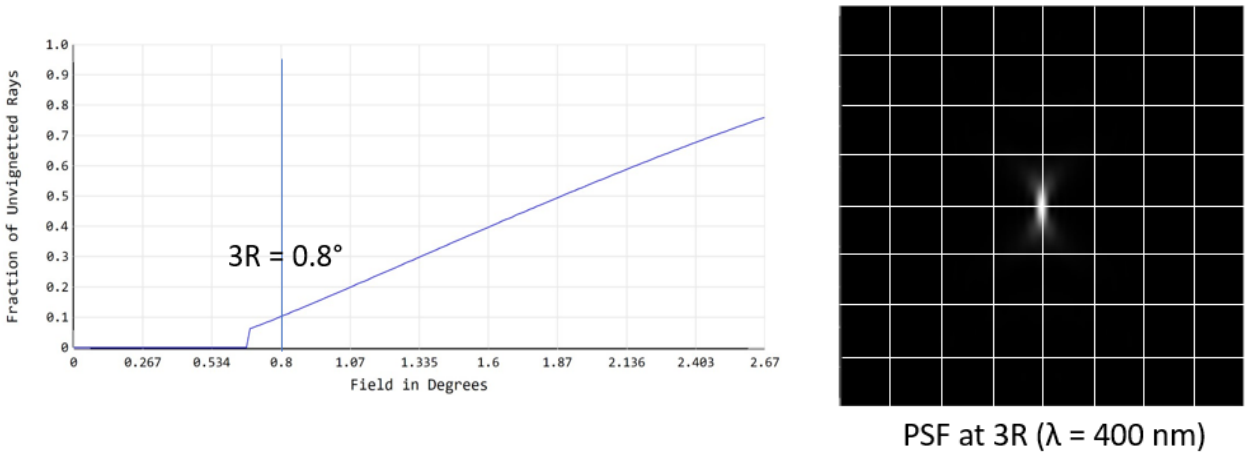

Figure 7. CODEX vignetting. On the left is the vignetting plot from CODEX model in Zemax. It shows the unvignetted beam at $3R_\odot$ reaches 10%. On the right is a PSF at $3R_\odot$, In the picture, each square is one CODEX super pixel. It shows the PSF at 400 nm is smaller than one CODEX super pixel: no degradation to spatial resolution.

It is found that the Lyot stop does not cut much diffraction anymore, because of majority of the diffraction is already suppressed by the focal mask and IO. However, we still have a Lyot mask in place in case it is needed. The final diffraction distribution on detector is shown in figure 8. It indicates that the required diffraction suppression – an order of magnitude lower than F-corona has achieved. The result has delivered for S/N assessment using the technology described by N. Reginald et al.[10]. The feedback is the stray light level is low enough to support needed S/N ratio for coronal temperature and velocity measurement.

It should be mentioned before completing this section: we understand that the longer EO length will reduce the diffraction efficiently. However, it will increase the vignetting at the same time. The vignetting is directly connected to the throughput and signal, CODEX can't afford to lose it. So, the decision was made to have a second stage and using the novel focal mask plus traditional IO mask to achieve the wanted diffraction suppression. This strategy turns out working well for CODEX.

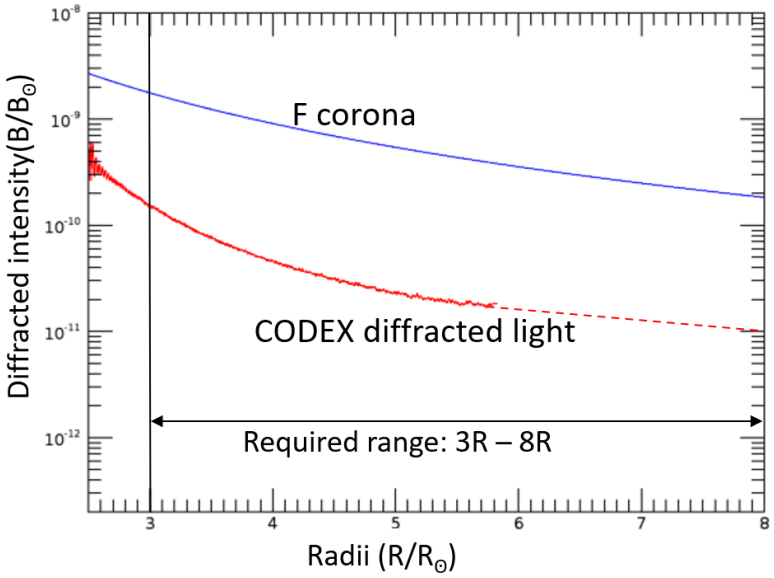

Figure 8. Simulated diffraction distribution compared to F-corona in the image plane. It shows that CODEX diffracted light is one order of magnitude lower than F-corona. Dashed red curve is extrapolated.

3. OPTICAL ALIGNMENT

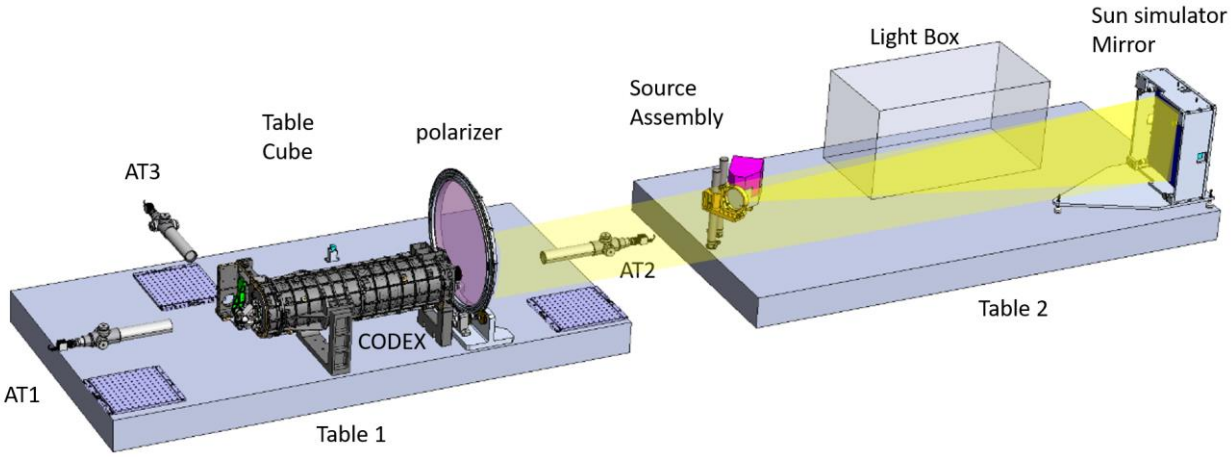

Figure 9. CODEX Optical alignment and test setup. On the table 1 is the CODEX instrument, and on the table 2 is the solar simulator. The polarizer on table 1 and light box on table 2 were not used for optical alignment. They are used for coronagraph characterization later.

Traditional coronagraph alignment uses optical alignment tools and metrology to complete the alignment and assembly first, and a specially designed solar simulator (requires precise apparent solar diameter and divergence) to test it. For CODEX alignment, the updated method is to test the diffraction during the alignment. CODEX has a focal mask in

telescope focal plane and a sharp ring in IO plane allowing us having an IO diameter just outside the ring. However, this implies that a higher alignment precision is required to position the focal mask and IO more accurately relative to the beam from solar simulator. Therefore, we have combined the two processes into one: using optical and metrology tools to align the coronagraph system as we normally do. Meanwhile, setup the coronagraph housing axis to the solar simulator axis, use the simulator to align the 5 key elements, such as EO, focal mask, etc. real time. The complete alignment and testing setup are shown in Figure 9.

The Solar simulator includes a source assembly and an off-axis-parabolic mirror. There is a circular mask at the focus of the parabola. The diameter of the mask ensures the beam after the parabola having the same angular extension of the Sun as seen from Earth. On CODEX housing, a number of metrology targets and cubes are pre-characterized using Coordinated Measuring Machine (CMM) (Faro Arm) and theodolite to indicate the mechanical axis. Three alignment telescopes AT1, AT2, and AT3 are mounted on stages with tip/tilt and XYZ adjustment.

The brief alignment procedure is the following:

1. Obtaining the simulator axis which is the simulator chief ray angle from the center of the FOV. This is the axis of the entire alignment. This is done by CMM.
2. To align AT1 and AT2 to simulator axis.
3. To align CODEX housing to simulator axis with Faro Arm and theodolite. The theodolite shoots pre-characterized reference cubes to align the housing orientation. The Faro Arm probe touches the targets to align the housing position.
4. The first element to be aligned is the EO (see figure 10). There is a pinhole at the center of both EO's front cap and back cap. These two caps are for alignment only. AT1 and AT2 are already aligned to coronagraph axis. The AT1 and AT2 looked at the front and back holes during the EO alignment until both holes centered on the reticles. This indicates the EO is aligned to coronagraph axis.
5. Aligning A1 aperture to the axis. Then moving the AT2 off the alignment axis. Note that the alignment telescopes are mounted on precision linear translation stages with long travel range to allow us moving them into and out with good repeatability. In addition, AT2 can look at AT1 to check if it is moved back to the previous position if necessary. A CMOS camera is used to real time monitor the diffracted light after A1 aperture for fine tuning the A1 position and EO position until the diffraction ring is minimized and uniformly around A1. Figure 11 (a) shows the optimized diffraction ring after A1, which indicates that EO and A1 is well aligned.
6. Install the telescope primary lens group and using the AT2 to align it.
7. Install the two fold mirrors. The individual mirror alignment is not that critical. The key is to make sure the beam angle and position out of the two folds are as designed. The two folds were aligned well at beginning. Unfortunately, one of the fold mirror (F2) was moved from its aligned position during stake due to mirror mount fabrication error. This error does not have impact on diffraction suppression but causes problem for geometric optical alignment for the last lens group and the detector.
8. Insert the A0 Stop at the A0 image plane to block the scattered light from the sawtooth edge of the A0 aperture. It is flashed with the front surface of EO.
9. The diffraction suppression is performed successfully as planned. Figure 11 (b) displays the residual diffraction in telescope focal plane. The focal mask is glued to the field lens, and IO disk is glued to a fused silica flat. They work great and provide easy alignment access. Figure 11 (b) shows that the diffraction ring at telescope focal plane is uniformly distributed around the focal mask, which implies that the occulter position is optimized for diffraction suppression. The diffraction is further suppressed in IO plane and the sharp diffraction ring in Figure 6 is completely blocked by the IO. Unfortunately, some scattered light is leaked through the gaps between EO and the spider pylons due to mechanical fabrication is not as precise as expected. An effort has been made to use covers to block the gaps. Fortunately, the diffraction patterns after covers are localized. In the area without the diffraction that is introduced by the cover edge, the total stray light (including both diffracted and scattered light) meets the requirement: the background brightness is an order of magnitude lower than F-corona. The detailed calibration is beyond the scope of this paper (see Casti et al., 2024b in preparation).

10. The diffraction ring at the Lyot stop is so low, the CMOS detector is not able to detect. It is not a surprise; it agrees with the diffraction analysis. Because the first order diffraction at A1 created by the EO is effectively suppressed by the focal mask and IO.
11. The last optical group is the relay lens group. The mechanical housing is not able to accommodate the lens group shift due to F2 error. We have aligned to the optimized position that the housing allows. This does not affect image quality much in the FOV we are most interested: 3 $R_\odot$ to 8 $R_\odot$.
12. Detector alignment has the same problem, The housing does not have enough margin to place the center of the camera chip to the center of FOV.
13. The final image is shown in Figure 12. The object is an air force target. It was inserted to the focus of a Questar telescope. The Questar is back illuminated to send a collimated beam to CODEX. The telescope output beam angle was tip/tilted to different angles to different CODEX fields. The image of the air force target shows the spatial resolution in $3R_\odot$ to $8R_\odot$ range meets the MTF requirement, which is the 36 cycles / mm. It also shows even at the field that is very close to inner FOV cutoff, the spatial resolution still meets the requirement. Nevertheless, occulted shadow is off the detector center. The image quality is also evaluated using Point Spread Function (PSF). the 36 lines / mm is equivalent to 51.2" (0.014°) RMS PSF size. Figure 13 shows the PSFs at $4.5R_\odot$[11] at 4 different orientations. They are meet the requirement. It is noted that the size of PSF on the left (c) is larger than that on the right. This is mainly due to the misalignment of the relay lens group due to the mechanical limitation.

The alignment section is ended with a picture of completely aligned CODEX in Figure 14.

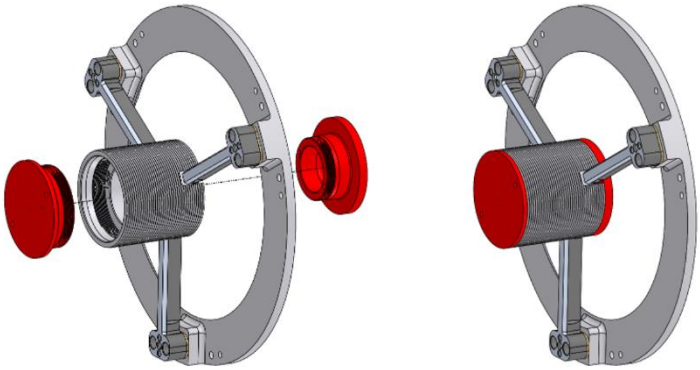

Figure 10. External occulter and its spider pylons. The front and back caps with pinholes at the center are for alignment purpose only.

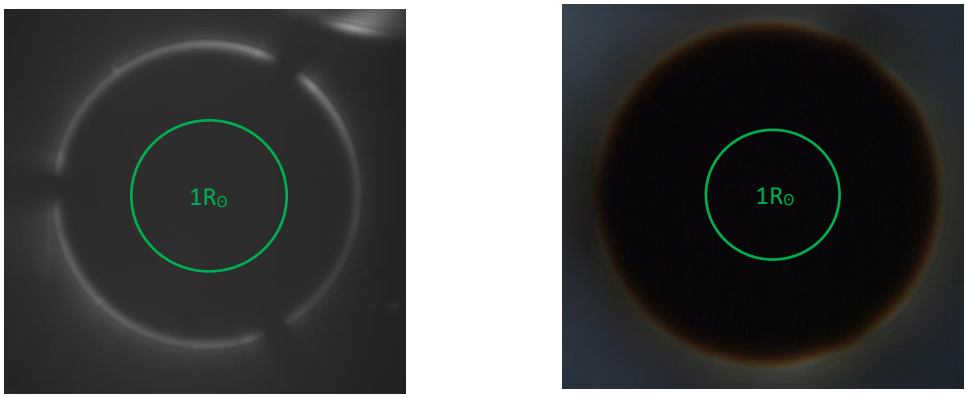

(a) (b)

Figure 11. The diffraction patterns. (a) diffraction ring after A1 aperture (note light in upper right corner is GSE artifact); (b) at telescope focus after focal mask installed demonstrating clear reduction.

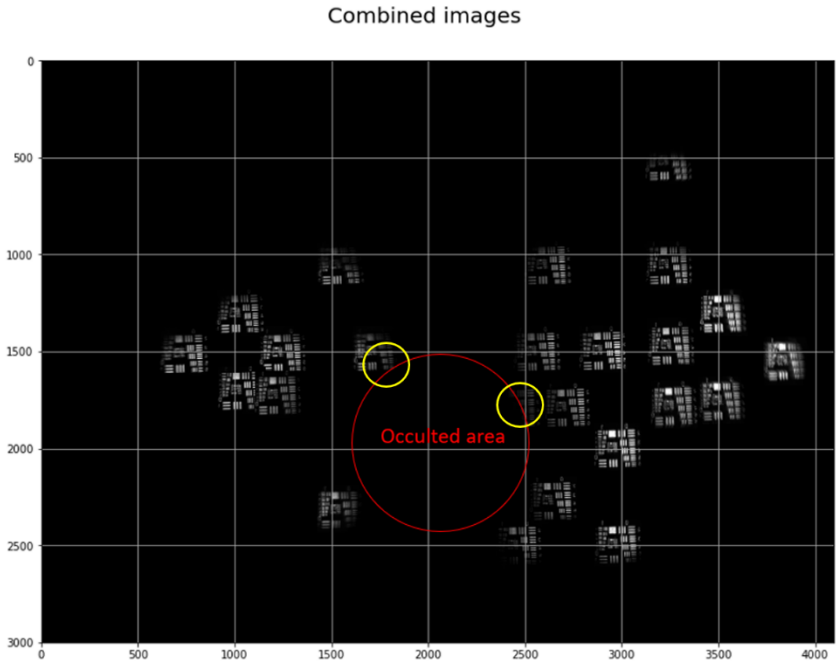

Figure 12. Combined air force target images. One image was taken at a time. All frames are digitally added to make the map. All individual images of the target meet the MTF requirement, except the one on the far right. Even for fields that are close to inner FOV cutoff, circled yellow, the requirement is still met. The red circle is occulted area.

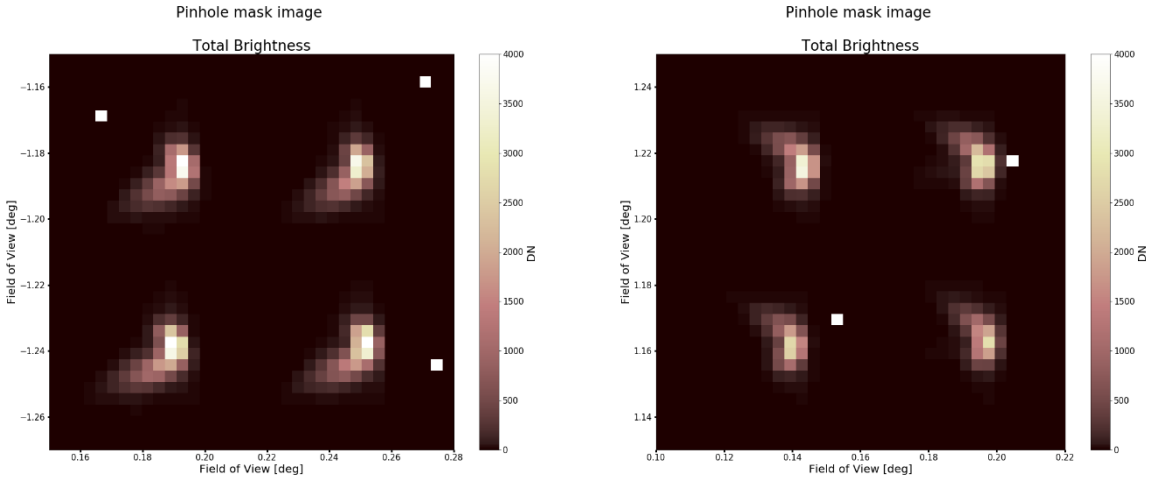

(a) (b)

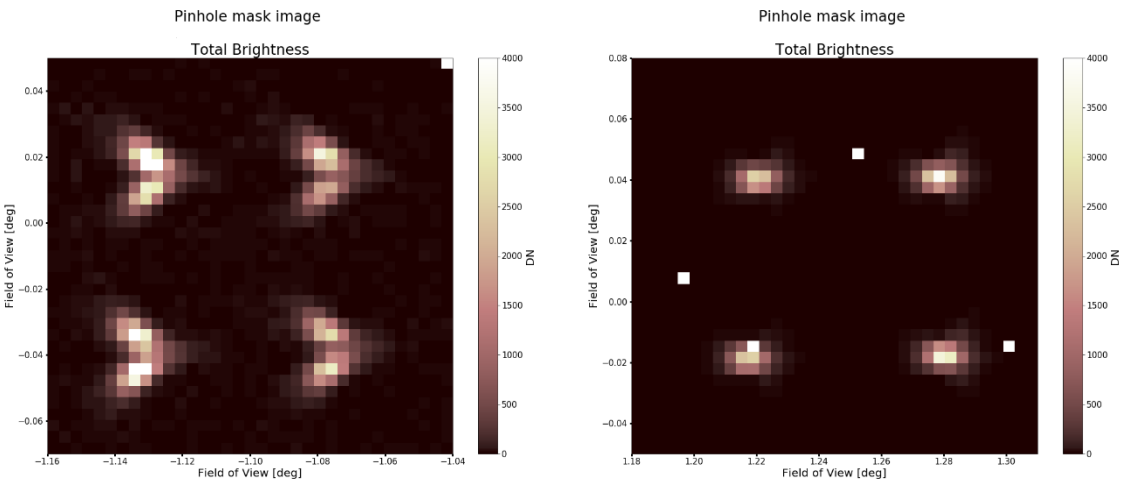

(c) (d)

Figure 13. PSF on detecter. The object for each image is a pinhole mask with 4 pinholes as 4 point sources. All 4 images are at $4.5R_{\odot}$ radially from center of the Sun. Orientation wise: (a) On top of Sun center, (b) At bottom of Sun center, (c) On the left of Sun center, (d) On the right of Sun center.

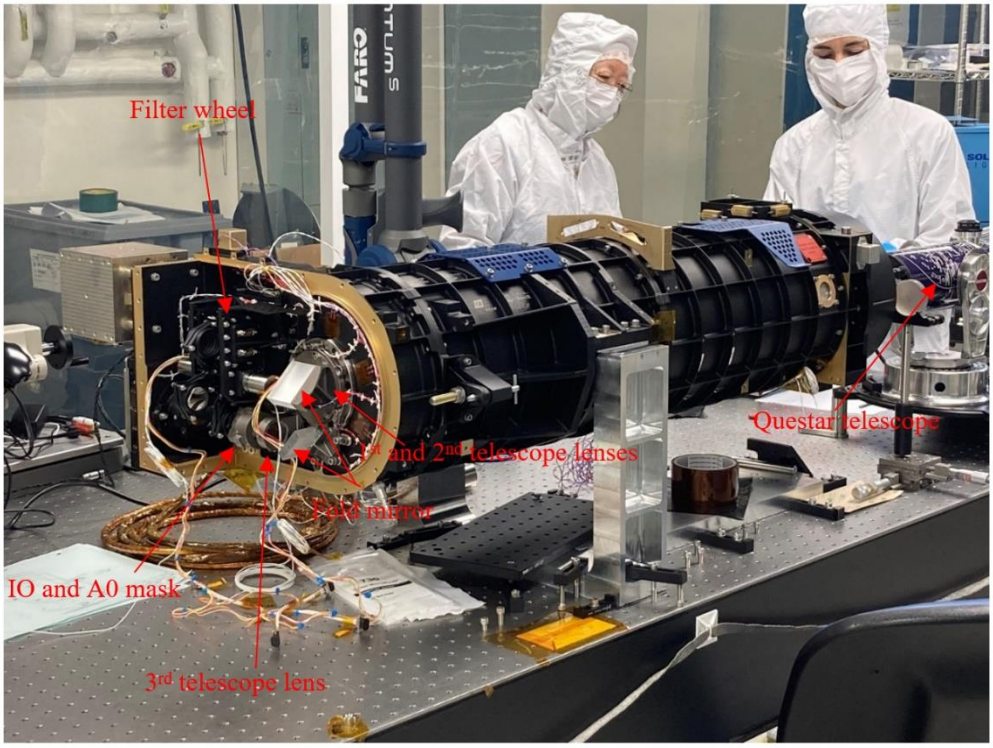

Figure 14. Completely aligned coronagraph undergoes the spatial resolution test using a Questar telescope.

4. CONCLUSION

Coronagraph optics has been well-designed to meet all requirements for coronal electron temperature and velocity measurement. A novel focal mask has been introduced to effectively cutoff the diffracted light in an estimated ≥ 1 order of magnitude. Combining traditional optical alignment with the real time diffraction monitoring works well for this alignment. For the first time we can monitor how the occulters or apertures are aligned with the diffraction and scattering in real time. It not only cuts off stray light more efficiently, but also avoided the number of test iterations. At the end, CODEX was successfully built and all key requirement related to the science are met.

During the integration of the optics, 2 main challenges arose. The first one concerns the combination of fold mirror mounts mounting error and tight adjustment range for the last lens group and camera. Small misalignment resulted in the Field of view off the center of camera. The second one concerns the interface between the support pylons and the EO. This interface is extremely critical, and a slight misalignment yielded additional straylight into the system. The result of this was a slightly elevated straylight in a localized area. A more detailed discussion of this is in Casti et al., 2024(b) (in preparation)[12].

There are some key lessons learned that are important to share. First, ensure the adjustment range for key optical elements is enough to handle any misalignment issues. Second, check the stray light residual at IO plane in simple lab setup before designing the IO mask. Then design IO pattern accordingly. Finally, the traditional way to hold IO is to use pylon(s), automatically blocking the EO pylon scattering. We have changed it to bond IO mask to a clear substrate. This design change could be the reason we have seen more leakage around the pylons.

CODEX will be launched in September of 2024 as an external payload of the International Space Station. The optical design has been improved significantly from image quality to stray light suppression to S/N ratio compared to the prototype, BITSE. We are looking forward to seeing a scientific breakthrough from CODEX.

ACKNOWLEDGMENTS

This work was supported by NASA ROSES NNH18ZDA001N-HTIDS funds. All KASI authors (Y.-H. K., J.-H. B., S.-C. B., K. C., S. C., J. K., S.-H. P., J. P., D. S., and H. Y.) were supported by KASI grants 2024-1-810-03 and 2024-1-850-02.

REFERENCES

[1] Gopalswamy, N., Newmark, J., Yashiro, S., P. Mäkelä, P., Reginald, N., Thakur, N., Gong, Q., Kim, Y.-H., Cho, K.-S., Choi, S.-H., et al., "The balloon-borne investigation of temperature and speed of electrons in the corona (bitse): mission description and preliminary results," Solar Physics 296(1), 15 (2021).

[2] Newmark, J. S., Gopalswamy, N., Kim, Y. H., Viall, N. M., Cho, K. S. F., Reginald, N. L., Bong, S. C., Gong, Q., Choi, S., Strachan, L., and Yashiro, S., "The Coronal Diagnostic Experiment (CODEX)," in [AGU Fall Meeting Abstracts], 2020, SH028–0011 (Dec. 2020).

[3] Brueckner, G., Howard, R., Koomen, M., Korendyke, C., Michels, D., Moses, J., Socker, D., Dere, K., Lamy, P., Llebaria, A., et al., "The large angle spectroscopic coronagraph (lasco) visible light coronal imaging and spectroscopy," The SOHO mission, 357–402 (1995).

[4] Howard, R. A., Moses, J., Vourlidas, A., Newmark, J., Socker, D. G., Plunkett, S. P., Korendyke, C. M., Cook, J., Hurley, A., Davila, J., et al., "Sun earth connection coronal and heliospheric investigation (secchi)," Space Science Reviews 136, 67–115 (2008).

[5] Nelson Reginald, Jeffrey Newmark, Lutz Rastaetter, "Statistical Error Analysis on White-light Filter Ratio Experiments to measure Electron Parameters," Solar Physics, 296:146, (2021). https://doi.org/10.1007/s11207-021-01887-1

[6] Marta Casti, et al. "Polarimetric characterization of the Coronal Diagnostic EXperiment (CODEX)," SPIE proceeding (2024)

[7] Heesu Yang, Kyuhyoun Cho, Su-Chan Bong, Seonghwan Choi Maria S. Madjarska, Yeon-Han Kim, Nelson Reginald, Jeffrey Newmark "Feasibility Study of Measuring Degree of Linear Polarization of the Solar F-Corona Using Filter Observations on the COronal Diagnostic EXperiment," Solar Physics 298:57 (2023).
[8]
[9] Max Born and Emil Wolf, [Principles of Optics], Pergamon Press, 6th edition, 333-334 (1987)
[10] Qian Gong, Natchimuthuk Gopalswamy, Jeffrey Newmark, "Innovative Compact Coronagraph Approach for Balloon-borne Investigation of Temperature and Speed of Electrons in the corona (BITSE)," Proc. SPIE 11116 111160F (2019), doi: 10.1117/12.2530408
[11] Nelson Reginald, Jeffrey Newmark, Lutz Rastaetter, "A Technique to Measure Coronal Electron Density, Temperature, and Velocity Above 2.5$R_\odot$ from Sun Center Using Polarized Brightness Spectrum," Solar Physics, 928:73, (2023). https://doi.org/10.1007/s11207-023-02160-3
[12] Casti M. et al, "CODEX geometric optical-performance and its impact on coronagraph science" in International Conference on Space Optics—ICSO 2024, in preparation.
[13] Casti M. et al, "CODEX solar coronagraph calibration," 2024b, in preparation.